AUV FORMATIONS ACHIEVED BY VIRTUAL POTENTIALS TRAJECTORY PLANNING IN A SIMULATED ENVIRONMENT

Matko Barisic*, Zoran Vukic*, Nikola Miskovic*, Boris Tovornik**

**University of Zagreb, Croatia*
Faculty of Electrical Engineering and Computing,
Laboratory for Underwater Systems and Technologies

***University of Maribor, Slovenia*
Faculty of Electrical Engineering and Computer Science

Abstract: This paper explores the forming-up, robustness of the ensuing formation and coordinated movement of autonomous, non-communicating submerged vehicles (AUV) planning their trajectories using a virtual potential fields method. The behavior and characteristic merits and problems of the proposed scheme, which plans the trajectory on the basis of AUV kinematics is tested in 2D simulations. A brief commentary on further avenues of research and improvement in order to make the method applicable to hardware-in-the-loop usage is given.

Keywords: Autonomous mobile robots, Trajectory planning, Gradients, Robot kinematics, Robot navigation

1. INTRODUCTION

Trajectory planning for autonomous underwater vehicles (AUV) is one of the key challenges which stand in the way of wide-spread commercial use of AUVs. Most missions would benefit significantly and usher in a new era of human presence in the underwater environment if AUVs could be programmed and guided to work in a coordinated manner. Difficulties in need of overcoming if such coordinated control is to be realized, in part arise from the naval-architectural and engineering constraints characteristic of AUVs. However, a much more significant problem is the inability of communication between cooperating AUVs. Due to this communication blackout, or at the very best severe bandwidth restriction, complete autonomy must be assured in the programmatic construction of the trajectory planning method.

However, such a trajectory planning method, running on embedded hardware as but one of the many hard-real-time modules of a hierarchical control system [ref], draws up high levels of processor commitment In order to reduce the number of layers in such a hierarchical system and to dispense with the greatest number of interdependencies and links which would have to be periodically checked and thereby induce overhead in the processor cycle, the trajectory planner should possess cross-level design features. Therefore, a trajectory planner based on the virtual potential method was developed by Barisic et. al (2006, 2007a, 2007b).

Section 2 defines the additions to the mathematics of the method in (Barisic et al. 2006, 2007a, 2007b) in order to assure forming behavior, proposing two solutions to the formation problem. Section 3 presents the results of simulations in comparison with the action of the algorithm in (Barisic et al. 2006, 2007a, 2007b) which does not explicitly include formation support, and the comparison of the two methods, and also proposes avenues for further research by presenting challenges and instances of suboptimal behavior. Section 4 concludes the paper.

2. ASSURING FORMATIONS BY MODIFYING THE VIRTUAL POTENTIALS METHOD

A trajectory planner for AUVs must be stable, energy efficient, have robust, certifiable and tested collision avoidance. In the context of multiple AUV working and moving in concert, a coordinated trajectory planner must in addition rely as much as possible on sensing rather than on communication (Barisic et al. 2006, 2007a, 2007b). Implementation-wise, such a trajectory planner must be implemented as well designed, safe, fast, bug-free code that is multi-threaded. It must run on a hard-real-time operating system that must assure that the multi-threading built into the code of the trajectory planner certifiably and recurrently runs fast enough, and while sharing the same hardware resources in parallel to other, sensing, DSP and feature extraction threads that assure the interaction between the trajectory planner and an nondeterministic, dynamic environment.

Although a significant number of researchers have tackled this problem area, this paper builds on a virtual potential method approach such as the ones in (Fiorelli et al. 2004; Mureau et al., 2003; Örgen et al., 2003). More properly, this work builds on the foundation of (Barisic et al., 2006, 2007a, 2007b). However, care is taken at this stage of the research to provide computational feedback that could at a later date be used to analytically explore the stability using insights from (Fax and Murray, 2003; Meshabi, 2004; Olfati-Saber and Murray, 2002, Sepulchre et al., 2005).

The greatest benefit of the virtual potential method is that it represents a strong case of cross-layer design, that it is intuitively understood and that the stability is assured by the conservative nature of the system (Barisic et al. 2006, 2007a, 2007b).

The method itself is based on the addition of virtual potentials, which produce a total potential field of a region of the problem space (wherein $\vec{p}$ is situated):

$$E(\vec{p}) = \sum_i f_{obj(i)}(\vec{p}(k)) \quad (1)$$

Wherefrom follows the formula for the original force of attraction or repulsion of features in the potential field:

$$\vec{F}_{orig}(k) = \max_i \left[E(\vec{p}_{AUV}(k)) - E(\vec{p}_{\varepsilon i}(k))\right] \angle \left(\arg\max_i \left[E(\vec{p}_{AUV}(k)) - E(\vec{p}_{\varepsilon i}(k))\right] \cdot \gamma\right) \quad (2)$$

Introducing the conservationism-breaking friction force according to Barisic et al. (2007a, 2007b):

$$\vec{F}_{fric}(k) = \xi \cdot \left|\vec{v}(k-1)\right| \angle \pi + \arg(\vec{v}(k-1)) \quad (3)$$

Results in the total:

$$\vec{F}_c(k) = \text{bound}\left(\vec{F}_{orig}(k) - \vec{F}_{fric}(k), F_{max}\right) \quad (4)$$

From which follows the formula for the set-point velocity in vector form:

$$\vec{v}(k) = \text{bound}\left(\frac{T}{2}\left(\vec{F}(k) + \vec{F}(k-1)\right) + \vec{v}(k-1), v_{max}\right) \quad (5)$$

In eqs. 1 – 5, the following are used uniformly:
- E is the virtual potential,
- $f_{obj(i)}$ are the PDFs of obstacles and other features of the problem space,
- $\vec{p}(k)$ with appropriate indices designate points in the problem vector space, at time index k,
- $\vec{F}_{orig}(k)$ is the directional potential-induced "original" force attracting or repulsing the AUV at k,
- $\vec{F}_{fric}(k)$ is the force of virtual viscose friction introduced to stabilize the planned trajectory (for explanation see Barisic et al. 2006, 2007a, 2007b),
- $\vec{F}_c(k)$ is the virtual controlling force,
- $\vec{v}(k)$ is the set-point velocity of the AUV at time index k

In order to fine-tune this approach to apply it to a real AUV, which is an expensive technological tool, there is significant need for simulation in order to arrive at the optimal values for a number of purely method-specific, implementation-independent tunable numerical parameters. An optimal set-up of such parameters, which can be performed in an out-of-water simulation environment is instrumental. This needs to be carefully arranged before implementing such an optimized method itself in a real craft. It needs to be kept in mind that it is highly likely that on a real craft further modifications can be expected. This mostly arise from the need to compensate for non-ideal or non-linear craft dynamics, and to employ caveats in interfacing the trajectory planning with actuator-layer control.

The simulation depends on further numerical trapezoidal integration of the set-point velocity:

$$\vec{p}_{AUV}(k+1) = \frac{T}{2}\left(\vec{v}(k) + \vec{v}(k-1)\right) + \vec{p}_{AUV}(k-1) \quad (6)$$

The PDFs (Barisic et. al 2006, 2007a, 2007b) characterizing detected environment- and mission-specific obstacles, are defined for:

1. a rectangular obstacle PDF – f_{orth}

$$f_{orth}(\vec{p}) = e^{\frac{A^+}{r(\vec{p})^2}} - 1 \quad (7)$$

Where:
- A^+ is the repulsive ponder of the obstacle (positive potentials are attributed to repulsive action), a method-specific independent parameter,
- $r(\vec{p})$ is *the characteristic radius* (as explained in Barisic et al. 2007a, 2007b)

2. a circular obstacle PDF, f_{circ}

$$f_{circ}\left(\vec{p}\right) = \mathrm{e}^{\frac{A^{+}}{\left(\left\|\vec{p}-\vec{p}_{obs}\right\|-r_0\right)^2}} - 1 \qquad (8)$$

Where:
- r_0 is the radius of the obstacle.

3. an elliptical obstacle PDF, $f_{ellipse}$

$$f_{ellipse}\left(\vec{p}\right) = \mathrm{e}^{\frac{A^{+}}{d\left(\vec{p}\right)^2}} - 1 \qquad (9)$$

Where:
- $d\left(\vec{p}\right)$ is the distance from the ellipse defined by the obstacle to the point at which the PDF is evaluated:

$$d\left(\vec{p}\right) = \left\| \begin{bmatrix} \frac{a^2}{t+a^2} \\ \frac{b^2}{t+b^2} \end{bmatrix} \cdot\cdot \vec{p} - \vec{p} \right| \qquad (10)$$

Where:
- $\cdot\cdot$ is used to denote element-wise multiplication and
- t is the largest numerical solution of the quartic polynomial:

$$\left(t+a^2\right)^2\left(t+b^2\right)^2 - a^2u^2\left(t+b^2\right)^2 - b^2v^2\left(t+a^2\right)^2 = 0 \qquad (11)$$

4. a goal-point PDF, f_{GP}

$$f_{GP}\left(\vec{p}\right) = -A^{-} \cdot \mathrm{e}^{-\frac{\left|\vec{p}-\vec{p}_{GP}\right|^2}{2\sigma^2}} \qquad (12)$$

Where:
- $\vec{p}_{GP}$ are the coordinates of the goal-point
- σ is the reach of the goal-point, determining how far the attractive influence of the goal-point extends in the theater of operations. This is a method-specific independent parameter.
- A^{-} is the attractive ponder of the goal-point, a method-specific independent parameter.

In work following the research presented in Barisic et al. (2006, 2007a, 2007b), a simulated environment was set-up in which multiple maneuvering AUVs would be able to detect one another at some finite radius r_{det}. If another AUV from the group was detected (henceforth "*foreign agent*"), it was also included in influencing the recumbent potential in the space surrounding the AUV which was running the trajectory planner (henceforth the "*viewpoint agent*"). In order to assure the collision-avoidance between the viewpoint agent and the foreign agent, the foreign agent is firstly a circular obstacle.

However, in order to assure formative behavior, the foreign agent was regarded by the viewpoint agent as a PDF which features local minima. The local minima are places that attract the viewpoint agent while it is on approach to the global goal-point, so that in traveling to the goal-point, the viewpoint agent would do so in formation with the foreign agent.

It is to be assumed that if the foreign agent is actually running the same trajectory planning algorithm, the mutual combined action of such local minima will attribute to the agents moving in concert, in predefined formation, towards the goal-point.

Two distinct PDF-s attributed to foreign agents will be tested in the course of simulation.

5. The gamma-function based foreign agent PDF, $f_{FA\gamma}$

$$f_{FA\gamma}\left(\vec{p}\right) = f_{circ}\left(\vec{p}, \vec{p}_{FA}\right) + \sum_{i=1}^{n_{SA}+1} f_{lattice}^{(i)}\left(\vec{p}\right) \qquad (13)$$

Where:
- $f_{circ}\left(\vec{p}, \vec{p}_{FA}\right)$ is the circular-obstacle PDF centered on the foreign agent,
- $f_{lattice}^{(i)}\left(\vec{p}\right)$ is the compound PDF of attractive lattices which define preferable or allowable directions of approach to a formation with the foreign agent,
- n_{SA} is the number of foreign agents the viewpoint agents perceives; The +1 addition to the sum over lattices is introduced since the viewpoint agent has to include *itself* in the future formation that it is trying to enter in with foreign agents.

The $f_{lattice}^{(i)}$ are compound potential distribution functions of n_{SA}+1 elliptical attractive lattices. These feature a minimum at the closer of the two foci of each ellipse that defines the shape of the negative-potential lattice to the foreign agent. The $f_{lattice}^{(i)}$ is calculated by assigning it the value of a Gaussian distribution function at δ_i, the displacement along the normal to the major axis of the defining ellipse of the lattice, as per fig. 1. The standard deviation of the Gaussian σ, is the third of the width of the ellipse d measured along the normal to the major axis passing through the relevant point, as per fig. 1. The mode of the Gaussian, is determined by the γ distribution with shape parameter k = 2, and scale parameter θ calculated from the eccentricity of the elliptical lattice e (which itself depends on r_S – the sensing radius, and the r_I – the preferred inter-agent formation distance) according to fig. 2. The γ distribution is evaluated along the axis x mapped to the major axis of the ellipse according to $x = 10 \cdot \lambda \cdot l^{-1}$, where λ is the point of projection of the viewpoint agent's position onto the major axis, as per figure 1.

Note that the ellipses (lattices) are defined as having major axes rotated about the foreign agent by multiples of $2 \cdot \pi/(n_{SA}+1)$. The nearer foci of the ellipses are defined as being at the distance of r_I away from the center of the foreign agent. The ellipses' apsides lie on the r_S-radius circle around the foreign agent.

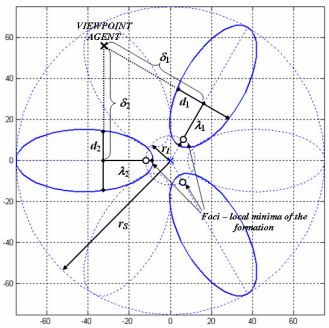

Figure 1: Construction of the elliptical lattice and parameters s, d, λ and δ in the 2D problem space

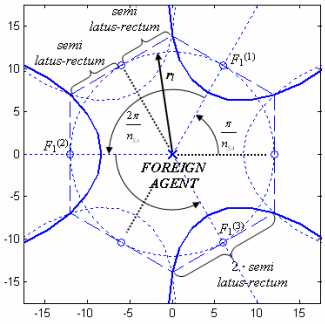

Figure 2: Detail of the construction

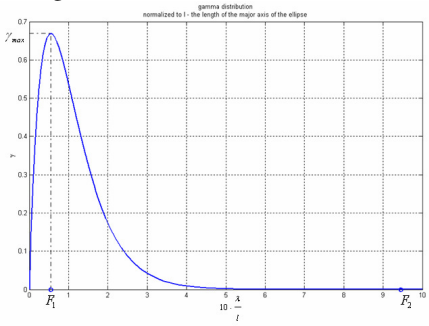

Figure 3: Mode (ponder) of the Gaussian potential distribution as a gamma-distribution function of the λ

$$f_{lattice}^{(i)} = -\frac{A_l^-}{\gamma_{max}}\gamma(\lambda)\cdot \mathrm{e}^{-\frac{9\cdot\delta^2}{2d^2}} \qquad (14)$$

Where:
- A_l^- is the attractive ponder of the local minimum which determines the preferred position of the viewpoint agent w.r. to the foreign agent,
- γ_{max} is the mode of the γdistribution,
- δ is the length of the normal to the i-th lattice's major axis through the viewpoint agent,
- d is the width of the ellipse at parameter λ (arrived at by considering the eccentricity and the semi-latus rectum, which are all calculated from r_l and r_S)
- $\gamma(\lambda)$ is the value of the γdistribution at λ (scaled in accordance with $10\cdot\lambda\cdot l^{-1}$):

$$\gamma(\lambda,k,\theta) = \left[10\frac{\lambda}{l}\right]^{k-1}\cdot\frac{\mathrm{e}^{-\frac{\left[10\frac{\lambda}{l}\right]}{\theta}}}{\theta^k\Gamma(k)} \qquad (15)$$

Where:
- Γ is the incomplete gamma-function,
- k is the shape parameter, which is an independently settable parameter (the value of 2 was used throughout the research presented in this paper)
- θ is the scale parameter, calculated as:

$$\theta = \frac{5\cdot(1-e)}{k-1} \qquad (16)$$

Where:
- e is the eccentricity of the ellipses defining the attractive lattices.

A view (the third dimension being the potential axis "above" the 2D problem space) of an example of a foreign-agent gamma-distribution-based PDF for the interaction of 3 agents is given below (this occurs when the viewpoint agent observes 2 additional foreign ones within r_S of itself – itself is the third):

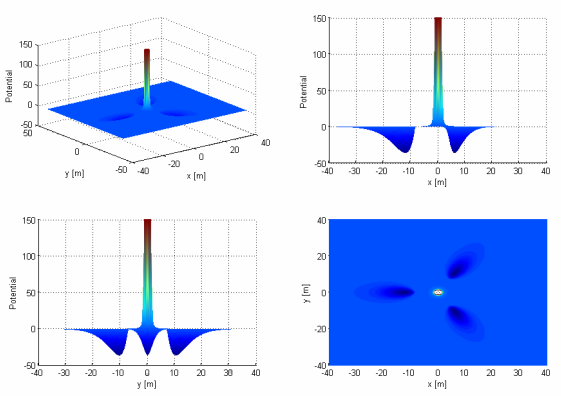

Figure 4: An example of a three-latticed gamma-distribution-based foreign-agent PDF

6. The Gaussian based foreign-agent PDF f_{Fag}

$$f_{FA\gamma}(\bar{p}) = f_{circ}(\bar{p},\bar{p}_{FA}) + \\ +\sum_{i=1}^{n_{SA}+1} f_{gauss}^{(i)}\left(\bar{p}-\bar{p}_{FA}-\bar{p}_{lm}^{(i)},\sigma,A^+\right) \qquad (17)$$

Where
- $f_{gauss}^{(i)}\left(\bar{p}-\bar{p}_{FA}-\bar{p}_{lm}^{(i)},\sigma,A^+\right)$ is the PDF of the i-th Gaussian local minimum situated symmetrically about the position of the foreign agent, $\bar{p}_{FA}$, and parameterized by the deviation σ and depth A^+.

A view (the third dimension being the potential axis "above" the 2D problem space) of an example of a foreign-agent Gaussian PDF for the interaction of 3 agents is given below:

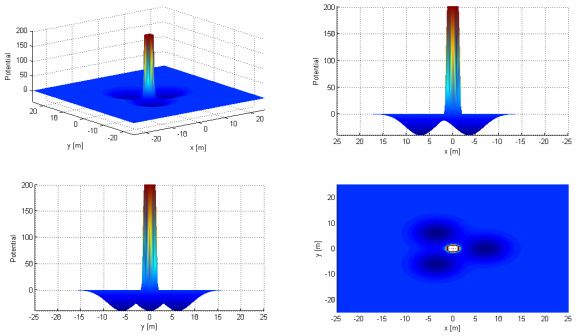

Figure 5: An example of a three-latticed Gaussian foreign-agent PDF

Both of these foreign-agent PDFs change dynamically, when more foreign agents encounter the formation including the viewpoint agent (enter the r_S-vicinity of the viewpoint agent). Also, foreign agents may leave the r_S–vicinity of the viewpoint agent if an obstacle is encountered (some foreign agents may choose to circumnavigate the obstacle by turning either down the port or the starboard side of the obstacle). Additional instability might be introduced by the fact that if foreign agents are running the same algorithm, they might attribute to the viewpoint agent (which to them is a "foreign agent") a foreign-agent PDF with a different number of lattices. This occurs since by "seeing farther", the agent in question might be "seeing" another foreign agent which the original viewpoint agent doesn't see. This is the problem of sensing agents within non-overlapping sensor radii of two or more agents sailing in formation.

3. SIMULATION RESULTS

The first experiment explores the trajectory-planning results of the algorithm proposed in Barisic et al. 2006, 2007a, 2007b in comparison to trajectories planned by the use of both methods presented in Section II. The setup of the area of operations is very basic: an uncluttered area with one centrally positioned global goal-point for all agents. There are four agents starting from various portions of the area of operations greater than their sensing radius.

Figures 6 to 8 present the comparison of the trajectories planned with the three methods.

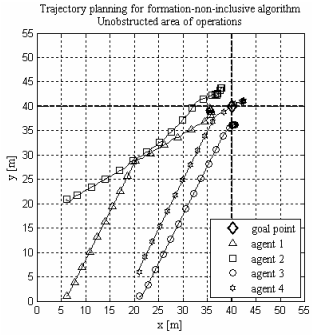

Figure 6: Trajectories in an unobstructed environment with a formation-non-inclusive algorithm

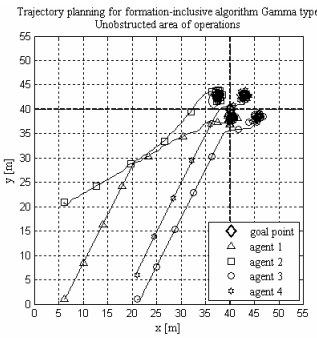

Figure 7: Trajectories in an unobstructed environment with the Gamma-distribution-type agent PDFs

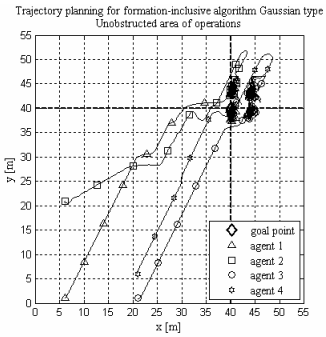

Figure 8: Trajectories in an unobstructed environment with the Gaussian-type agent PDFs

The second experiment explores the comparative benefits of the two introduced formation-inclusive vs. the formation-non-inclusive method of Barisic et al. 2006, 2007a, 2007b, when there is an obstacle in the way of the agents towards the global goal-point. Four agents start off in a rectangular formation, but their sensing ranges are insufficient for each of them to register all three other agents. Thereby, the optimal formation for four thus position agents would be two adjoined equilateral triangles (similar to the finishing formation in figure 8). This is intentional, in order to explore formation-breakup and –rejoining after encountering the "watershed"-type obstacle.

Figures 9 to 11 present the comparison of the planned trajectories. The obstacle is an elongated rectangular "watershed". It is positioned so that either circum-navigating it to port or starboard might be optimal for certain agents, depending on their starting positions.

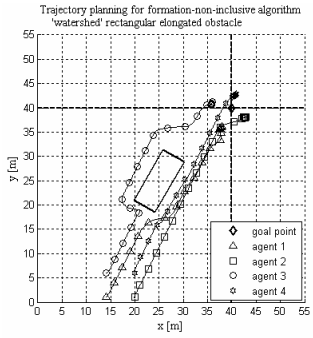

Figure 9: Trajectories in an obstructed environment with a formation-non-inclusive algorithm

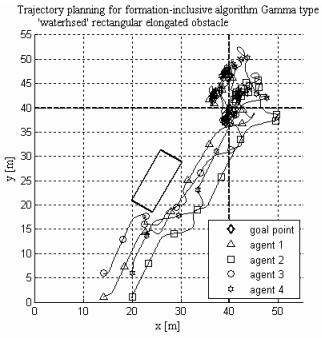

Figure 10: Trajectories in an obstructed environment with the Gamma-distribution-type agent PDFs

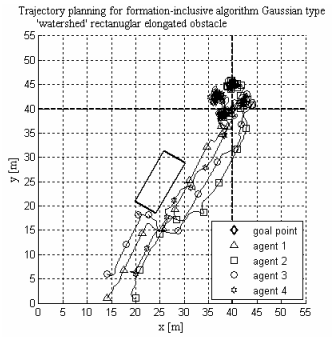

Figure 11: Trajectories in an obstructed environment with the Gaussian-type agent PDFs

The third experiment gives a comparison of the scenario used in the second experiment, but only comparing the performance of two formation-inclusive methods. The difference between the trajectories arises due to an extension of the sensor range of individual agents.

Figures 12 and 13 present the comparison of planned trajectories by the use of the two proposed methods.

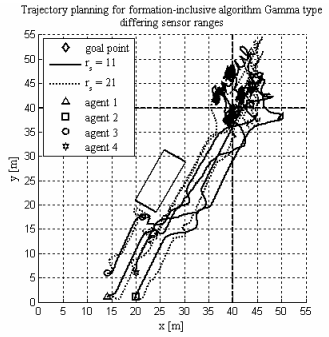

Figure 12: Comparison of the Gamma-distribution-type agent PDF method with a step-up in sensor range of individual agents

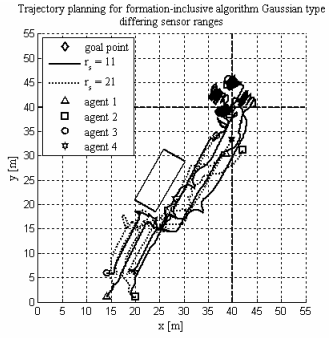

Figure 13: Comparison of the Gaussian-type agent PDF method with a step-up in sensor range of individual agents

4. CONCLUSION

Both methods, proposed and mathematically introduced in Section II have been simulated. Both demonstrate an ability to provide for a formation-maintaining trajectory planning in a dynamic, previously unmapped environment (simultaneously sensed). The Gaussian PDFs demonstrate greater smoothness of the planned trajectory during the approach or "cruise" phase. Also, the calculation of the Gaussian-type local minima contribution to the potential map is than that of the gamma-distribution-type agent PDFs. Both of these factors combine to present the Gaussian PDFs as a clear choice for further development.

Both methods, even at this stage of development, have been shown to be BIBO stable. However, both exhibit a limit-cycle type "*parking creep*". The "parking creep" is the occurrence of "creeping" small circular parking orbits of each agent. The "creep" is introduced by the attractive influence of the goal point, and the circular orbits are an effect of all agents "tail-chasing" local minima of other agents within the sensor range. This will have to be explicitly addressed in further modifications to the trajectory planning algorithm. Filtering techniques need to be developed to eliminate suboptimal "jittery" behavior. Further precision on-goal-point is needed for mission profiles wherein specific action is required of AUVs upon reaching a predefined sub-area of the area of operations.

REFERENCES

Barisic, M., Vukic, Z. and Miskovic, N. (2006), "Design Of A Coordinated Control System For Marine Vehicles", *Proceedings of the 7th IFAC Conference on Manoeuvring and Control of Marine Craft*, Proceedings on CD

Barisic, M., Vukic, Z. and Miskovic, N. (2007a), "Kinematic Simulative Analysis of Virtual Potential Field Method for AUV Trajectory Planning", *Proceedings of the 14th IEEE Mediterranean Conference on Control* (*accepted*)

Barisic, M., Vukic, Z. and Miskovic, N. (2007b), "A Kinematic Virtual Potentials Trajectory Planner For AUV-s", *Proceedings of the The 6th IFAC Symposium on Intelligent Autonomous Vehicles* (*accepted*)

Fax, J. A. and Murray, R. M. (2003). "Information Flow and Cooperative Control of Vehicle Formations", *IEEE Transactions on Automatic Control,* **vol. 9**, pp. 1465-1476

Fiorelli, E. et al. (2004). "Multi-AUV Control and Adaptive Sampling in Monterey Bay", *Proceedings of the IEEE Autonomous Underwater Vehicles 2004: Workshop on Multiple AUV Operations,* pp. 134-147

Meshabi M. (2003). "State-Dependent Graphs", *Proceedings of the 42nd IEEE Conference on Decision and Control,* **vol. 3,** pp. 3058-3063

Mureau L., Bachmeyer R. and Leonard N. E. (2003). "Coordinated Gradient Descent: A Case Study of Langrangian Dynamics With Projected Gradient Information", *Proceedings of the 2nd IFAC Workshop on Lagrangian and Hamiltonian Methods for Nonlinear Control*

Ögren P., Fiorelli E., Leonard N. E. (2003), "Cooperative Control of Mobile Sensor Networks: Adaptive Gradient Climbing in a Distributed Environment", *IEEE Transactions on Automatic Control*, **vol. 9**, pp. 1292-1302

Olfati-Saber R. and Murray R. M. (2002). "Graph Rigidity and Distributed Formation Stabilization of Multi-Vehicle Systems", *Proceedings of the 41st IEEE Conference on Decision and Control,* **vol. 3**, pp. 2965-2971

Sepulchre R., Paley D. and Leonard N. E. (2005). "Graph Laplacian and Lyapunov Design of Collective Planar Motions", *Proceedings of the International Symposium on Nonlinear Theory and Its Application*